

Intermediate coupling model of cuprates: adding fluctuations to a weak coupling model of pseudogap and superconductivity competition

R.S. Markiewicz, Tanmoy Das, Susmita Basak, and A. Bansil
Physics Department, Northeastern University, Boston MA 02115, USA
(Dated: November 6, 2018)

We demonstrate that many features ascribed to strong correlation effects in various spectroscopies of the cuprates are captured by a calculation of the self-energy incorporating effects of spin and charge fluctuations. The self energy is calculated over the full doping range from half filling to the overdoped system. In the normal state, the spectral function reveals four subbands: two widely split incoherent bands representing the remnant of the two Hubbard bands, and two additional coherent, spin- and charge-dressed in-gap bands split by a spin-density wave, which collapses in the overdoped regime. The resulting coherent subbands closely resemble our earlier mean-field results. Here we present an overview of the combined results of our mean-field calculations and the newer extensions into the intermediate coupling regime.

Over the past few years evidence has been mounting that correlation effects in the cuprates are not as strong as previously thought and that these materials may fall into an intermediate coupling regime. If so, the transition to an insulator could be described in terms of Slater physics by invoking a competing phase with long-range magnetic order, rather than Mott physics requiring a disordered spin liquid phase with no double occupancy. The most striking evidence in this direction perhaps is the existence of quantum oscillations in underdoped cuprates associated with small Fermi surface pockets.[1, 2] Strictly, quantum oscillations have only been observed in strong magnetic fields, so that it is possible that the ordered phases are field-induced.[3] Nevertheless, it is clear that a phase with long-range order lies close in energy to the ground state. Additional evidence comes from the recent calculation of the magnetic phase diagram of the half-filled $t - t' - U$ model by Tocchio, *et al.*[4] They found that the ground state is either non-magnetic at small U or possesses a long-range magnetic order, except for a small pocket of spin-liquid phase at values of U and $|t'|$ too large to be relevant for the cuprates. Further, the high-energy spectral weight associated with the ‘upper Hubbard band’ decreases with doping too fast to be consistent with strong coupling (no double occupancy) models.[5, 6]

There have been a number of recent attempts to extend strong coupling calculations into the intermediate coupling regime. Yang, *et al.*[7] have introduced a phenomenological self energy that is similar to that of an ordered magnetic phase, but with a special sensitivity to the magnetic zone boundary. Paramekanti, *et al.*[8] have carried out variational resonant-valence bond (RVB)-like calculations where the requirement of no double occupancy has been relaxed. However, given that the ground state is close to being magnetically ordered, one could also approach intermediate coupling by including effects of fluctuations in a weak coupling scheme, where the lowest order (Hertree-Fock) solution already describes a long-range ordered state. This article presents an

overview of our ongoing work in this direction.[6, 9]

We begin with a brief recapitulation of the mean-field calculations, which by themselves can provide a good description of the doping dependence of the low-energy coherent part of the electronic spectrum. The model is nearly quantitative for electron-doped cuprates, where the competing magnetic order is known to be (π, π) antiferromagnetic over the full doping range. Such a model can describe many features of the hole-doped cuprates as well, even though the competing order[s] are known to be more complicated.[10, 11] Within this model, for electron-doped cuprates, the ground state at half-filling is an antiferromagnetic insulator, doping simply shifts the Fermi level into the upper magnetic band producing an electron pocket near $(\pi, 0)$, and the magnetization decreases with doping until magnetism collapses in a quantum critical point near optimal doping. This quantum critical phase transition in fact involves two Fermi surface driven topological transitions[12], the first near $x = 0.14 - 0.15$ where the top of the lower magnetic band crosses the Fermi level producing hole pockets near $(\pi/2, \pi/2)$, and a second transition near $x = 0.18$, where the hole and electron pockets recombine into a single large Fermi surface. The model has been able to describe angle-resolved photoemission (ARPES),[13, 14] resonant inelastic x-ray scattering (RIXS),[15] and scanning tunnelling microscopy (STM)[16] spectra, and the unusual pairing symmetry transition with doping seen in penetration depth measurements[17]. Recently, quantum oscillations were observed in electron doped cuprates at several dopings, showing a crossover from the hole pocket at lower dopings to the large FS at the highest doping.[18] Furthermore, the areas of the FS pockets measured by quantum oscillations are well predicted by the model for the electron doped case, while hole doped cuprates remain controversial in this aspect.

Fluctuations modify the above picture in several ways. First, in two-dimensional materials, critical fluctuations are well-known to eliminate long-range order and drive the antiferromagnetic transition temperature to zero in

accord with the Mermin-Wagner theorem, so that over a wide range of temperatures only a pseudogap remains. [The observed Néel order is driven by small deviations from isotropic two-dimensional magnetism.] These fluctuations can be accounted for in a self-consistent renormalization scheme[19], and are necessary to describe the response of the system at higher temperatures. Fluctuations also modify the low-temperature physics at higher energies, leading to the high-energy kink or the waterfalls seen in ARPES[20–22], effects of the ARPES matrix element notwithstanding[23–27]. We have recently introduced the quasiparticle-GW (QP-GW) scheme to account for these fluctuations.[6, 9] In this way, we have been able to describe the doping dependence of the optical spectra[28–30], including both the ‘Slater-like’ collapse of the midinfrared peak with doping and the ‘Mott-like’ persistence of a high-energy peak into the overdoped regime. The model also quantitatively accounts for the anomalous spectral weight transfer to lower energies with doping in the cuprates.[6]

In a GW-scheme, the self-energy is calculated from a variant of the lowest-order ‘sunset’ diagram, a propagator dressed by the emission and reabsorption of a bosonic operator,

$$\Sigma(\mathbf{k}, \sigma, i\omega_n) = \frac{1}{2} \sum_{\mathbf{q}, \sigma'} \eta_{\sigma, \sigma'} \int_{-\infty}^{\infty} \frac{d\omega_p}{2\pi} \Gamma(\mathbf{k}, \mathbf{q}, \omega_n, \omega_p) G(\mathbf{k} + \mathbf{q}, \sigma', i\omega_n + \omega_p) \text{Im}[W^{\sigma\sigma'}(\mathbf{q}, \omega_p)], \quad (1)$$

Here, σ is the spin index. $W \sim U^2\chi$ denotes the interaction, which involves the Hubbard U and the susceptibility χ in the random phase approximation (RPA)[31], and Γ is a vertex correction.[32] $\eta_{\sigma, \sigma'}$ gives the spin degrees of freedom, which takes value of 2 for transverse spin and 1 for longitudinal and charge susceptibility. The model involves three Green’s functions, the bare G_0 , the dressed G given by Dyson’s equation $G^{-1} = G_0^{-1} - \Sigma$, and an internal Green’s function G_{int} which will be described further below. A number of different variants of the GW scheme can be constructed, depending on the specific Green’s function used in evaluating the G and the W in the convolution integral of Eq. 1.[33] Using the bare G_0 in both G and W in the so-called ‘ G_0W_0 ’ scheme corresponds to lowest order perturbation theory. Using the dressed G in both G and W (i.e. the GW scheme) leads to fully renormalized propagator and interaction corresponding to an infinite resummation of diagrams. However, this is still not the exact self-energy because of the missing vertex corrections. In fact, GW scheme often gives worse results than G_0W_0 version when the vertex corrections are omitted. Bearing all this in mind, our approach is an intermediate one, in that it is based on the convolution of an intermediate coupling Green’s function and interaction. In this spirit, we first calculate the self-energy of Eq. 1 by using a parameterized $G = G_{int}(Z)$, and then calculate W_{int} exactly based on this G_{int} , and determine

the renormalization parameter Z self-consistently.

More specifically, we write G_0 in terms of *the unrenormalized LDA dispersion*. Note that our tight-binding hopping parameters are not free parameters, but are the best representation of the first-principles LDA dispersion. All renormalizations, giving rise to the experimental results, are embedded in the computed Σ . W is the sum of the RPA spin plus charge susceptibilities calculated using G_{int} rather than G_0 . The key lies in the choice of G_{int} . Our strategy is to construct the best one parameter model for $G_{int}(Z)$ with Z chosen to minimize $G - G_{int}$. [$G_{int} = G$ of course yields the full GW .] To motivate our choice, we recall that the main effect of Σ at low energies is to renormalize the dispersion from the LDA values to those observed in experiments (e.g., ARPES). This renormalization, which amounts to a factor of 2-3, is relatively modest in that the mass does not diverge, and depends weakly on k . [34] That is, approximately

$$\epsilon_{\mathbf{k}, ARPES} = Z\epsilon_{\mathbf{k}, LDA}. \quad (2)$$

Hence, we choose perhaps the simplest G_{int} which reproduces this dispersion renormalization, $G_{int}^{-1} = G_0^{-1} - \Sigma_{int}$, with $\Sigma_{int} = (1 - Z^{-1})\omega$, so that

$$G_{int}(\mathbf{k}, \omega) = \frac{Z}{\omega - Z\epsilon_{\mathbf{k}, LDA} + i\delta}. \quad (3)$$

The above expression refers to the paramagnetic phase, but the extension to a magnetically ordered phase is straightforward where G , χ , and Σ become (2×2) tensors for the (π, π) antiferromagnetic order.[6, 31]

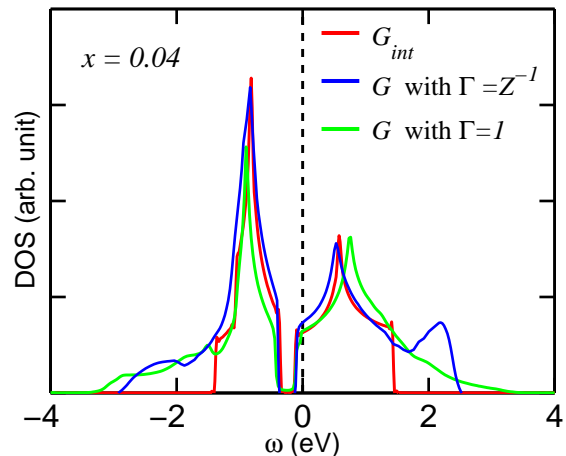


FIG. 1: DOS computed from G_{int} is compared with the fully dressed DOS with a vertex correction $\Gamma = 1/Z$ and without the vertex correction (i.e. $\Gamma = 1$) at a representative doping of $x=0.04$ as discussed in the text.

Self-consistency is obtained by choosing Z such that the low energy dispersion is the same for G and G_{int} . This is illustrated in Figs. 1 and 2. Fig. 1 compares the density-of-states (DOS) associated with G_{int} (red line)

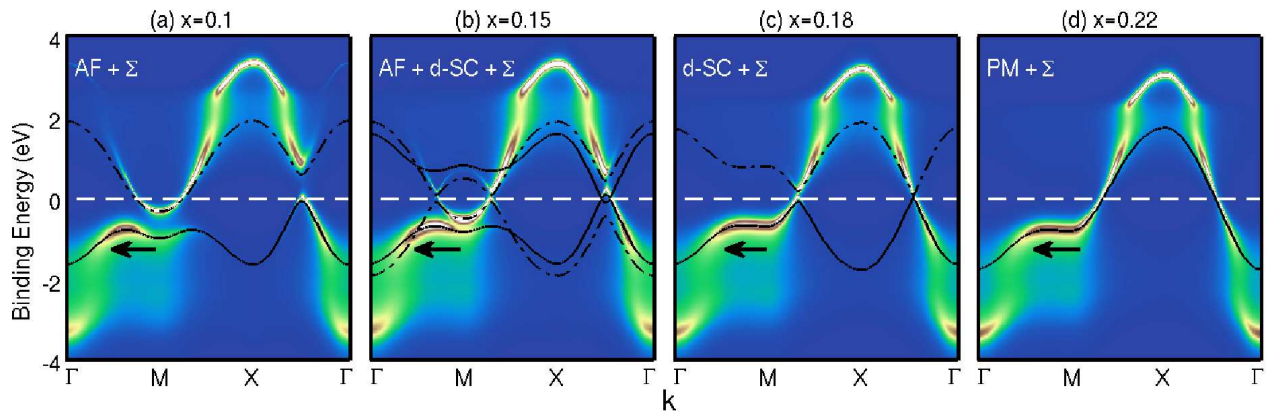


FIG. 2: Spectral intensity plots along the high symmetry lines for antiferromagnetic (AF) ($x = 0.10$), AF+ d -wave superconducting (SC) ($x = 0.15$), d -SC ($x = 0.18$), and the paramagnetic (PM) ($x = 0.22$) states. Full self-energy Σ is included in all cases. Antiferromagnetic order parameters are computed self-consistently.[6] Self-energy is computed including the antiferromagnetic gap, but does not incorporate the low energy superconducting gap. Black lines depict the dispersions that enter into G_{int} , but the corresponding spectral weight of the band is not shown for simplicity[14]. An artificially large value of superconducting gap ($\Delta = 30$ meV) is used so that the effects of superconductivity can be visible on the energy scale of the figure.[35] Arrows mark the start of the high-energy kink or the waterfall in the spectrum below the Fermi energy.

and G , either with (blue line) or without (green) a vertex correction in the antiferromagnetic state. As discussed further below, G and G_{int} -dressed DOSs clearly match well with each other in the low energy regime where both spectra show the spin density wave dressed upper and lower magnetic bands, consistent with our earlier mean-field results[14, 17, 35]. At high energies, however, G_{int} fails (by construction) to reproduce the incoherent hump features associated with precursors to the upper and lower Hubbard bands.

Fig. 2 compares the spectral weights, $A = -Im(G)/\pi$, with the corresponding dispersions $\epsilon_{\mathbf{k},int}$ (black lines) that enter into G_{int} . As noted earlier, the latter provide a very good fit to the low energy coherent features for the entire doping range in electron doped $Nd_{2-x}Ce_xCuO_4$ (NCCO). Self-consistency ensures that G_{int} provides the best approximation to the full G . As an added benefit, Z in general renormalizes $\epsilon_{\mathbf{k},int}$ to values close to those found in our earlier mean-field studies[14, 17, 35]. The obtained self-consistent values of Z decrease almost linearly with doping, as seen in ARPES[36]. In this way, the QP-GW model reproduces the results of our earlier mean-field calculations in the low energy region, while revealing new physics at higher energies [e.g., the waterfall effect].

We now comment on some applications of the present QP-GW model. The waterfall physics seen in ARPES spectra of the cuprates is a direct consequence of the self-energy correction, which introduces a peak in scattering at intermediate energies below as well as above the Fermi level as seen in Fig. 2.[27] This scattering splits the spectrum into a low-energy coherent part and a high-energy incoherent region. While the near-Fermi-level dispersion changes substantially as the magnetic and the

superconducting phases evolve with doping, the overall energy regime of the waterfall phenomenon remains fairly doping independent (marked by arrows in Fig. 2), consistent with experiments.[21] In the pseudogap region ($x = 0.10$, Fig. 2(a)), the resulting ‘four band’-like structure (two magnetic bands and the two Hubbard bands) agrees well with cluster[37] and quantum Monte Carlo calculations[38]. Near optimal doping d -wave superconductivity coexists with the antiferromagnetic state in a uniform phase[17, 35] resulting in further splitting of the coherent bands as seen in Fig. 2(b). The coherent bands approach the Fermi level with increasing spectral weight as the pseudogap collapses at a quantum critical doping near $x = 0.17$ in both the electron and hole doped case[10]. On the other hand, the Hubbard bands move towards higher energy as the doping increases and the spectral weight associated with these bands decreases, consistent with optical spectra.[28, 30]

Notably, the lifetime broadening of the quasiparticle states originates from magnetic scattering in the QP-GW model. This broadening has a non-Fermi liquid form with a significant linear-in-T component, particularly near the Van Hove singularity (VHS).[9] Furthermore, in describing broadening of ARPES features in the superconducting state in our earlier mean-field model, we phenomenologically introduced an elastic small angle scattering contribution of similar non-Fermi-liquid form[35, 39, 40]

$$\Sigma''(\omega) = sgn(\omega)C_0 \left[1 + \left(\frac{\omega}{\omega_0} \right)^p \right]. \quad (4)$$

Here $C_0 = 100$ meV and $\omega_0 = 1.6$ eV are determined from a fit to the ARPES energy distribution curves (EDCs). The exponent p is of physical significance in determining quasiparticle character[41]. We found that

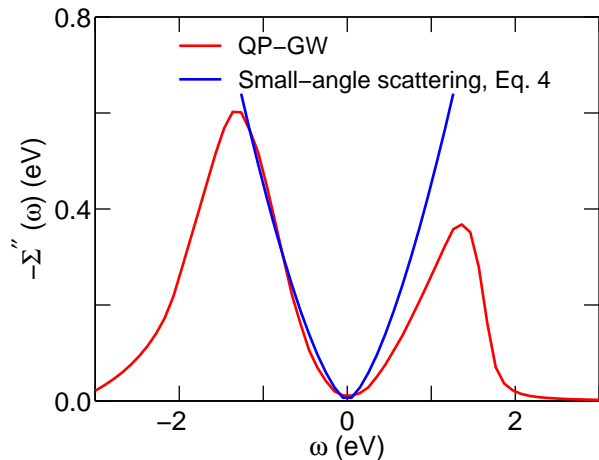


FIG. 3: Imaginary part of the self-energy for NCCO (red line) is compared with the form used in Eq. 4. Note that the model small angle scattering formula was only applied to filled states, $\omega < 0$.

$p = 3/2$ [35, 39, 40] applies for electrons as well as hole doped cuprates in reproducing the ARPES spectra and quasiparticle interference (QPI) pattern seen in scanning tunneling spectroscopy. This scattering is particularly important in that it allows a finite spectral weight near the Fermi level even in the presence of a pseudogap, thereby revealing the leading edge superconducting gap at all momenta[10, 35]. In Fig. 3 we show that the imaginary part of the self-energy computed from Eq. 1 above reproduces this phenomenological form very well in the low-energy region, both in magnitude and T -dependence, indicating that magnon scattering underlies the anomalous exponent $p = 3/2$.

We emphasize that in our QP-GW model the bare dispersion is taken directly from LDA, and the self-consistently determined Z renormalizes this into a dispersion which matches the bands seen in ARPES experiments. Hence, the model reproduces our earlier mean-field results, but with *fewer parameters*, since the dispersion is calculated self-consistently rather than being derived from experiment.

As noted above, the high energy features are absent in G_{int} . This is also clear from Eq. 3: If we integrate the spectral weight $A_{int}(\mathbf{k}, \omega)$ over all frequencies we get Z , not 1, so that G_{int} accounts for only the coherent part of G . The incoherent part of weight, $1 - Z$, is thus not accounted for. Clearly, this could be done straightforwardly by including a pair of broadened Lorentzians, but this will add additional parameters in the computation of the self-energy, not to mention associated vertex corrections. Therefore, we have chosen to first explore the QP-GW model without these complications. This is also the reason for calling our approach as QP-GW because it focuses on the QP part of the spectrum in evaluating G_{int} .

In order to better understand the susceptibility χ_{int} , a comparison with our earlier mean-field result, χ_{MF} is instructive. Since G_{int} differs from G_{MF} only by an overall multiplicative factor of Z , χ_{int} differs from χ_{MF} by a factor of Z^2 . This has important consequences. Fermi liquid theory requires that both the dispersion and the spectral weight be renormalized by interactions, and for a weakly k -dependent self energy, as in the present case, $Z_{disp} \simeq Z_\omega$. This is true for G_{int} and G , but $Z_\omega = 1$ for G_{MF} , which causes mean-field theory to overestimate the tendency towards instability. As the bandwidth decreases ($Z \rightarrow 0$), the density of states and susceptibility must increase as $1/Z$, in order to keep the total electron number fixed since there are no incoherent states in mean-field theory. Instability is controlled by the Stoner factor, $U\chi_0(\mathbf{q}, \omega = 0) = 1$. Since $\chi_0(\mathbf{q}, 0, MF) = \chi_0(\mathbf{q}, 0, LDA)/Z$, a small Z enhances the probability of instability. On the other hand, for G or G_{int} only the low-energy quasiparticle degrees of freedom contribute to the instability, as reflected in $\chi_0(\mathbf{q}, 0, int) = Z\chi_0(\mathbf{q}, 0, LDA)$. Hence, large fluctuations (small Z) actually reduce the probability of condensing into any one mode. Equivalently, if we rewrite the Stoner factor in terms of the LDA susceptibility, it becomes $U_{eff}\chi_{0,LDA} = 1$, with $U_{eff} = ZU$. Thus t and U should both be renormalized by factors of Z , leaving t/U invariant. In our mean-field treatment, we had to assume that the effective U was doping-dependent, and this Z -correction accounts for part of that doping dependence. .

It should be noted that an accurate calculation of the susceptibility and the resulting self-energy is fairly computer intensive as it involves a three-dimensional integral (k_x, k_y, ω) for χ_0 and a similar three-dimensional integral over χ 's for Σ . Fortunately, we find that Σ has only a weak k -dependence, so we need to calculate it only over a few k -points and use the average. Clearly, this is not a limitation of the model, and the full k -dependence could be calculated. However, this would make accurate self-consistent calculations substantially more time intensive. We have explored the use of a vertex correction for Σ , but the results are not too sensitive. We have typically taken $\Gamma = 1/Z$, which puts somewhat greater weight into the incoherent bands as seen by comparing blue and green curves at higher energies in Fig. 2.

The present scheme can straightforwardly incorporate the full k -dependence of the susceptibility based on a realistic material specific band structure.[11] This is important for delineating the nature of competing ordered phases, which are different for electron and hole doped cuprates. Moreover, our self-energy provides a tangible basis for going beyond the conventional LDA-based framework for realistic modeling of various highly resolved spectroscopies, providing more discriminating tests of theoretical models. In addition to the ARPES spectra discussed above, a note should also be

made in this connection of the optical spectroscopy,[6] STM [16, 42, 43], RIXS[15, 44], x-ray absorption spectroscopy (XAS)[45] and other inelastic light scattering spectroscopies[25, 46–48] to help piece together a robust understanding of the nature of electronic states in the cuprates and their evolution with doping.

In summary, we have shown that our intermediate coupling model of self-energy, which is based on the spin-wave dressing of the quasiparticles, can explain many anomalous features of the cuprates. At low energies, the model reproduces our mean field results for the coherent bands in ARPES,[27] optical,[6] and RIXS,[44] with self-energy corrections renormalizing the large widths of the LDA dispersions. At high energies, we obtain the waterfall features which represent a splitting off of the incoherent bands, precursors of the Mott gaps seen in ARPES and optical studies. In the underdoped regime, the coherent in-gap bands reproduce both the four-band behavior seen in quantum cluster calculations and the magnetic gap collapse found in the mean-field calculations and a variety of experiments. These results clearly suggest that the cuprates can be understood within the intermediate coupling regime with an effective U value substantially smaller than twice the bandwidth.

This work is supported by the US Department of Energy, Office of Science, Basic Energy Sciences contract DE-FG02-07ER46352, and benefited from the allocation of supercomputer time at NERSC, Northeastern University's Advanced Scientific Computation Center (ASCC). RSM's work was partially funded by the Marie Curie Grant PIIF-GA-2008-220790 SOQCS.

-
- [1] N. Doiron-Leyraud, C. Proust, D. LeBoeuf, J. Levallois, J.-B. Bonnemaïson, R. Liang, D. A. Bonn, W. N. Hardy, and L. Taillefer, *Nature (London)* **447**, 565 (2007).
- [2] N. E. Hussey, M. Abdel-Jawad, A. Carrington, A. P. Mackenzie, L. Balicas, *Nature* **425**, 814 (2003).
- [3] A.D. Beyer, M.S. Grinolds, M.L. Teague, S. Tajima, and N.-C. Yeh, arXiv:0808.3016, accepted for publication in *Europhysics Letters*.
- [4] L.F. Tocchio, F. Becca, A. Parola, and S. Sorella, *Phys. Rev. B* **78**, 041101 (2008).
- [5] A. Comanac, L de Medici, M. Capone, and A. J. Millis, *Nature Physics*, **4**, 287 (2008).
- [6] Tanmoy Das, R. S. Markiewicz and A. Bansil, arXiv:0807.4257.
- [7] K.-Y. Yang, T.M. Rice, and F.-C. Zhang, *Phys. Rev. B* **73**, 174501 (2006).
- [8] A. Paramekanti, M. Randeria, and N. Trivedi, *Phys. Rev. B* **70**, 054504 (2004).
- [9] R. S. Markiewicz, S. Sahrakorpi, and A. Bansil, *Phys. Rev. B* **76**, 174514 (2007).
- [10] Tanmoy Das, R. S. Markiewicz, and A. Bansil, *Phys. Rev. B* **77**, 134516 (2008).
- [11] R.S. Markiewicz, J. Lorenzana, G. Seibold, and A. Bansil, unpublished.
- [12] Tanmoy Das, R.S. Markiewicz and A. Bansil, *J. Phys. Chem. Solids*, **69**, 2963 (2008).
- [13] N.P. Armitage, D.H. Lu, C. Kim, A. Damascelli, K.M. Shen, F. Ronning, D.L. Feng, H. Eisaki, Z.-X. Shen, P.K. Mang, N. Kaneko, M. Greven, Y. Onose, Y. Taguchi, and Y. Tokura, *Phys. Rev. Lett.* **88**, 257001 (2002).
- [14] C. Kusko, R. S. Markiewicz, M. Lindroos, and A. Bansil, *Phys. Rev. B* **66**, 140513(R) (2002).
- [15] R.S. Markiewicz and A. Bansil, *Phys. Rev. Lett.* **96**, 107005 (2006).
- [16] Tanmoy Das, R.S. Markiewicz, and A. Bansil, *Phys. Rev. B* **77**, 134516 (2008).
- [17] Tanmoy Das, R. S. Markiewicz and A. Bansil, *Phys. Rev. Lett.* **98**, 197004 (2007).
- [18] T. Helm, M.V. Kartsovnik, M. Bartkowiak, N. Bittner, M. Lambacher, A. Erb, J. Wosnitza, and R. Gross, *Phys. Rev. Lett.* **103**, 157002 (2009).
- [19] R.S. Markiewicz, *Phys. Rev. B* **70**, 174518 (2004).
- [20] F. Ronning, K. M. Shen, N. P. Armitage, A. Damascelli, D. H. Lu, Z.-X. Shen, L. L. Miller, and C. Kim, *Phys. Rev. B* **71**, 094518 (2005).
- [21] J. Graf, G.-H. Gweon, K. McElroy, S. Y. Zhou, C. Jozwiak, E. Rotenberg, A. Bill, T. Sasagawa, H. Eisaki, S. Uchida, H. Takagi, D.-H. Lee, and A. Lanzara, *Phys. Rev. Lett.* **98**, 067004 (2007).
- [22] Z.-H. Pan, P. Richard, A.V. Fedorov, T. Kondo, T. Takeuchi, S.L. Li, Pengcheng Dai, G.D. Gu, W. Ku, Z. Wang, H. Ding, arXiv:0610442v2.
- [23] M. Lindroos, S. Sahrakorpi, and A. Bansil, *Phys. Rev. B* **65**, 054514 (2002).
- [24] M. C. Asensio, J. Avila, L. Roca, A. Tejada, G. D. Gu, M. Lindroos, R. S. Markiewicz, and A. Bansil, *Phys. Rev. B* **67**, 014519 (2003).
- [25] A. Bansil, M. Lindroos, S. Sahrakorpi, and R. S. Markiewicz, *Phys. Rev. B* **71**, 012503 (2005).
- [26] S. Sahrakorpi, M. Lindroos, R. S. Markiewicz, and A. Bansil, *Phys. Rev. Lett.* **95**, 157601 (2005).
- [27] Susmita Basak, Tanmoy Das, Hsin Lin, J. Nieminen, M. Lindroos, R.S. Markiewicz, A. Bansil, *Phys. Rev. B* **80**, 214520 (2009).
- [28] Y. Onose, Y. Taguchi, K. Ishizaka, and Y. Tokura, *Phys. Rev. Lett.* **87**, 217001 (2001).
- [29] Y. Onose, Y. Taguchi, K. Ishizaka, Y. Tokura, *Phys. Rev. B* **69**, 024504 (2004).
- [30] S. Uchida, T. Ido, H. Takagi, T. Arima, Y. Tokura and S. Tajima *Phys. Rev. B* **43**, 7942 (1991).
- [31] G. Vignale and M. R. Hedayati, *Phys. Rev. B* **42**, 786 (1990).
- [32] The self energy is calculated in Matsubara space and continued analytically as $i\omega_n \rightarrow \omega + i\delta$ where δ is a positive infinitesimal.
- [33] Giovanni Onida, Lucia Reining, and Angel Rubio, *Rev. Mod. Phys.* **74**, 601 (2002).
- [34] R.S. Markiewicz, S. Sahrakorpi, M. Lindroos, Hsin Lin, and A. Bansil, *Phys. Rev. B* **72**, 054519 (2005).
- [35] Tanmoy Das, R.S. Markiewicz, and A. Bansil, *Phys. Rev. B* **74**, 020506(R) (2006).
- [36] S. Sahrakorpi, R. S. Markiewicz, Hsin Lin, M. Lindroos, X. J. Zhou, T. Yoshida, W. L. Yang, T. Kakeshita, H. Eisaki, S. Uchida, Seiki Komiyama, Yoichi Ando, F. Zhou, Z. X. Zhao, T. Sasagawa, A. Fujimori, Z. Hussain, Z.-X. Shen, and A. Bansil, *Phys. Rev. B* **78**, 104513 (2008).
- [37] C. Gröber, R. Eder, and W. Hanke, *Phys. Rev. B* **62**, 4336 (2000).

- [38] M. Jarrell, Th. Maier, M. H. Hettler, A. N. Tahvil-darzadeh, Europhysics Letter, **56**, 563 (2001).
- [39] R. Hlubina and T. M. Rice, Phys. Rev. B **51**, 9253 (1995); R. S. Markiewicz, Phys. Rev. B **69**, 214517 (2004).
- [40] T. Dahm, P. J. Hirschfeld, L. Zhu, and D. J. Scalapino, Phys. Rev. B **71**, 212501 (2005).
- [41] N. S. Vidhyadhiraja, A. Macridin, C. Sen, M. Jarrell, and Michael Ma, Phys. Rev. Lett. **102**, 206407 (2009).
- [42] J. Nieminen, Hsin Lin, R. S. Markiewicz, and A. Bansil, Phys. Rev. Lett. **102**, 037001 (2009).
- [43] Jouko Nieminen, Ilpo Suominen, R. S. Markiewicz, Hsin Lin, and A. Bansil, accepted in Phys. Rev. B (2009).
- [44] Susmita Basak, Tanmoy Das, Hsin Lin, R. S. Markiewicz, and A. Bansil, Manuscript under preparation, APS March Meeting Abstract: Q41.00007 (2010).
- [45] Towfiq Ahmed, John J. Rehr, Joshua J. Kas, Tanmoy Das, Hsin Lin, R. S. Markiewicz, B. Barbiellini, and A. Bansil, Manuscript under preparation, APS March Meeting Abstract: Z40.00012 (2010).
- [46] Yoshikazu Tanaka, Y. Sakurai, A. T. Stewart, N. Shiotani, P. E. Mijnders, S. Kaprzyk, and A. Bansil, Phys. Rev. B **63**, 045120 (2001).
- [47] S. Huotari, K. Hmlinen, S. Manninen, S. Kaprzyk, A. Bansil, W. Caliebe, T. Buslaps, V. Honkimki, and P. Suortti, Phys. Rev. B **62**, 7956 (2000).
- [48] B. Barbiellini, A. Koizumi, P. E. Mijnders, W. Al-Sawai, Hsin Lin, T. Nagao, K. Hirota, M. Itou, Y. Sakurai, and A. Bansil, Phys. Rev. Lett. **102**, 206402 (2009).